sciendo

Environmental & Socio-economic Studies

DOI: 10.2478/environ-2019-0013

Environ. Socio.-econ. Stud., **2019, 7, 3: 1-13**

Original article

A geospatial approach to flash flood hazard mapping in the city of Warangal, Telangana, India

Aneesha Satya Bandi*, Shashi Meshapam, Pratap Deva

Department of Civil Engineering, National Institute of Technology, Warangal-506004, Telangana, India
*E–mail address (*corresponding author): aneeshatya@gmail.com*
ORCID iD: Aneesha Satya Bandi – https://orcid.org/0000-0002-1610-3069 ; Shashi Meshapam – https://orcid.org/0000-0001-8305-6832; Pratap Deva – https://orcid.org/0000-0002-6765-475X

ABSTRACT

Dense urbanization leading to uncontrolled transformations within settlements result in flash flooding with overflowing drains leading to a greater inconvenience for the public and damage to private properties. Hence mapping of flash floods would be useful in identifying the high-risk flood zones for disaster response and urban services, during emergencies with rainfall events of high intensity. This article aims to prepare a flood hazard map of Warangal Municipal Corporation (WMC) in Telangana State, India. WMC is chronically affected due to a rise in water levels resulting in flash floods, with an increase in encroachments. The factors considered in this study are rainfall (curve number), surface slope and surface roughness, type of soil, and distance to main channel, drainage density, and land use cover. To decide the relative weight of the impact of each flood causative factors an Analytical Hierarchical Process (AHP) was used. Accordingly, a composite Flood Hazard Index (FHI) has been derived by using the multiple-criteria decision-making tools by integrating these into a Geographical Information System (GIS). The Soil and Water Assessment Tool (SWAT) in Quantum GIS (QGIS), which is a hydrological model, was used to evaluate the projection of streamflow over the water basin and model parameters were optimized using water balance equations during calibration and validation periods.

KEY WORDS: Remote Sensing, GIS, Runoff, Multicriteria Decision Analysis, Analytical Hierarchical Process, Flood Hazard Index

ARTICLE HISTORY: received 11 March 2019; received in revised form 19 July 2019; accepted 18 August 2019

1. Introduction

The quick beginning of a flood with a brief span and a moderately high peak discharge is largely characterized as a flash flood. It happens quickly and is occasionally joined by landslides, bridge collapse, harm to structures, and fatalities. On the off chance, if the intensity of the rainfall surpasses the evaporation rate and infiltration capacity of the soil, surface runoff happens as a flash flood (ELKHRACHY, 2015). Increase in urbanization has been accounted to aggravate flooding by making ground surfaces impermeable, which decreases infiltration. Thus making settlements the obvious victims of natural hazards like flash floods, which could attack a city without pre-warning.

In the most recent years, a flood was forecasted by applying hydrologic and hydraulic models, which needed large-scale data that are not accessible. The utilization of GIS-based MCDA about flood hazard evaluation was uncommon before 2000. An outline of changes was presented by BLACK & BURNS (2002) in the estimation of flood hazard on Scottish waterways with a time line by re-examining the history of flood occurrence. Natural disasters are multidimensional phenomena with a spatial dimension, which makes GIS very applicative for such analysis (ZERGER, 2002; WANG ET AL., 2011; VAHIDNIA ET AL., 2010; PATEL & SRIVASTAVA, 2013; JAAFARI ET AL., 2014). As per (ALAGHMAND ET AL., 2010), a direct relationship exists between morphological & hydrological attributes in urbanization, diminished

infiltration, increase in frequency of the flood and increase in runoff. An early endeavour to use the applications of GIS in water-related mitigation issues was given in MEJA-NAVARRO ET AL. (1994). GIS was an incredible way perceived by CORREIA ET AL. (1999) to incorporate and investigate information from various sources about flood hazard mapping and it was used for diverse situations of urban development, re-enacting the results of different case studies. A GIS-based framework for rainfall-runoff modeling was worked out by SCHUMANN ET AL. (2000), while several parameters in their rainfall–runoff model (elevation, soil, land use, etc.) were incorporated by LIU ET AL. (2003), to appraise the average flow time in river basins and the spatial distribution of runoff. Flood vulnerability was connected with essential monetary exercises for specific study areas by VEEN & LOGTMEIJER (2005). The work of LIU ET AL. (2003) was expanded by FORTE ET AL., (2005) to divide a southern Italy peninsula into zones that were prone to flood risk. The historical major flood event in the year 1998 of Dhaka River basin in Bangladesh was re-modeled by (DEWAN ET AL., 2000) to create flood hazard maps, by processing historical data considering the segregate effect of geomorphology, elevation and Land Use Land Cover (LULC). Flood risk maps in Romania were generated by ALDESCU (2008), for the flood events of the years 2000, 2005 and 2006. KOEHLER & VOLCKENS (2011) interpreted that the resulting maps help the planners to give a visual way, to identify the source of a hazard and to look at the degree to which a risk is scattered all through a domain. To support the water management experts and flood mitigation FERNÁNDEZ & LUTZ (2010) used MCDA in the delineation of flood hazard zones for the Tucuman province (Argentina). A combined application of MCDA and GIS is helpful in the generation of flood risk maps (SOWMYA ET AL., 2015; WANG ET AL., 2011; GERL ET AL., 2014). DE SHERBININ ET AL. (2012) identified sensitive ecosystems and high flood risk regions by considering the impact of floods, by developing a net migration model. Many researchers used pairwise comparison, within analytic hierarchy process method (AHP) and geographical information systems (GIS) to assess flood hazard (EMMANOULOUDIS ET AL., 2008; SINHA ET AL., 2008; MEYER ET AL., 2009; CHEN ET AL., 2011) in order to incorporate the possible changes in climate and LULC over years into the assessing and management of flood and water resources. Multicriterian approaches were then later used by (OLOGUNORISA, 2003; SANYAL & LU, 2006; MANSOR ET AL., 2004) but these specialists did not consider the significance of each factor. So as to figure the relative weight of each factor, relationship among factors affecting the flood hazard must be considered. Direct method of rating (ZANGEMEISTER, 1971) and the pairwise comparison (KOELLE, 1975) are the two most popular techniques used for the estimation of the relative weight of each factor. During recent work (TEHRANY ET AL., 2013) ten parameters were included in the analysis and outlined the relative importance of every parameter, following statistical analysis. In TEHRANY ET AL. (2014) flood hazard was studied in Malaysia, enclosing the parameter distance from a river. As a standout, technique amongst the most prevalent methods of multi criteria decision-making, AHP has been broadly utilized (ZHU ET AL., 2015) in the GIS environment for generating flood hazard maps, with a decent level of precision. AHP is a semi-quantitative and multi criteria technique intended for portrayal of the hierarchy of a decision-making issue, which has increased wide application in predicting a flash flood, in landslide vulnerability analysis and in flood hazard estimation.

This article manages the first element of flood risk management, i.e. the definition of flood hazard areas in Warangal Municipal Corporation. The aim of this research was to map the Flood Hazard Index (FHI) for sites vulnerable to flash floods, using GIS and available spatial data sources, where mitigation measures are to be taken. A hierarchical structure through the AHP method was implemented to evaluate the factors considered whereas the analysis of the data, preparation of the urban flood-hazard map was carried out in the GIS environment to develop an integrated approach for the urban case study.

2. Methods and materials

2.1. Study area

Warangal Municipal Corporation (WMC), is a highly urbanized part of Warangal urban district, which lies between $17^0$46’ and $18^0$13’ (Fig. 1), with a population of 746594 as per 2011 census. The area for the most part, has a tendency to be dry without real changes in the temperature, which ranges from 34^0C to 42^0C. It gets very warm in the mid-year periods of April, May and June. The stormy season sets in Warangal city with the start of south-west rainstorms in the later part of June, and extends into September with the finish of the south-west tempest. The normal yearly rainfall of the region is 800 mm, with the extreme precipitation recorded in the long stretches of July, August and September consistently. The Kakatiya Canal is a noteworthy water supply source for irrigation and drinking water for Warangal city. Rain has

encouraged the use of tanks, wells and lakes, which require enough showers during the season, as some of the other sources of water supply for the city.

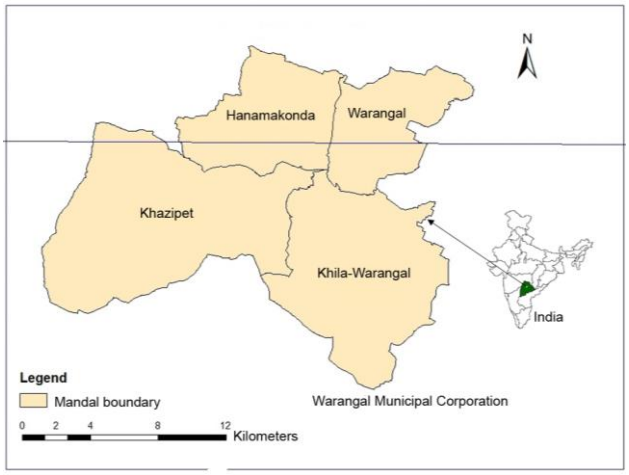

Fig. 1. Location map of the study area

The soils of Warangal city are classified as red earths, black soils (shallow to deep) and forest soils, which are rich in potash. Surface drainage shapes an essential viewpoint about Warangal city but the improper design or blockage to the natural drainage pattern has resulted in unhygienic conditions in the town, severe water logging and high vulnerability risk.

2.2. Data sets

In the context of this study, the collateral dataset such as Toposheets at 1:50,000 scale collected from Survey of India (SOI) was used for the preparation of the base maps and rainfall data for the years 1995 to 2005 was obtained from the Irrigation & CAD Department, Warangal, Government of Telangana. The Landsat 7 satellite data (https://earthexplorer.usgs.gov/), which is high-resolution (15 to 60 meter) multispectral data, were obtained for the year 2005 from the United States Geological Survey (USGS). The acquired satellite data was imported to ERDAS 2016 (https://www.hexagongeospatial.com/products/power-portfolio/erdas-imagine) to perform image classification. Important drivers of LULC change, which included thematic layers like demographic and soil data, were collected from the Chief Planning Office of Warangal municipality.

2.3. Flow sequence for calculating the flood hazard index

The sequence of operations in the methodology adopted is shown in Fig. 2, which is summarized as follows: the direction in which water will flow from a cell in consideration of its immediate surrounding cells yields the Flow Direction raster, which is created, directly from Digital Elevation Model (DEM). The flow accumulation raster is obtained from the flow direction raster where the number of cells upstream, accumulate into a cell of interest. From the flow direction and flow accumulation grids, the drainage network is created. Once the main channel is extracted from the drainage network, the distance from the main channel to the small order streams is calculated as the areas located close to a channel and flow accumulation path are more likely to get flooded (ELKHRACHY, 2015). Basin information is calculated from the stream network; later the drainage density is computed from the basin information and drain network. Once the main channel is extracted from the drainage network, the Euclidean distance is calculated in order to obtain the main channel distance to the small order streams.

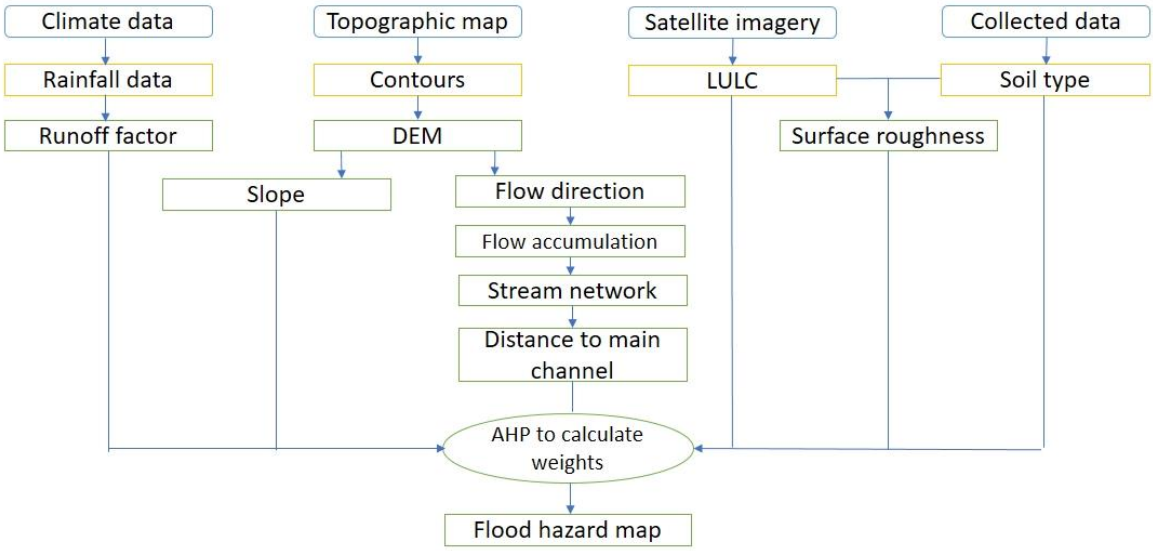

Fig. 2. Flow chart of the proposed methodology for flood hazard mapping

Model files of different inputs like the boundary of the study area, land use map, soil map, and weather data were prepared. The results were simulated using the above-mentioned physical parameters in the QSWAT environment where the physical processes associated with water movement can be studied. The model files of different inputs like the boundary of the study area, land use map, soil map, and weather data were given as input and hydrological parameters were simulated using the above-mentioned physical parameters in the QSWAT environment. Hydrological parameters are computed from the previous information. All the data was integrated into a GIS based multi-criteria decision event (OUMA & TATEISHI, 2014) analysis using AHP to obtain the flood hazard map.

2.4. Factors considered in the flood mapping

The likelihood of an event within a given time period of a potentially damaging phenomena and its area is characterized as a debilitating event called a hazard. At the point when a hazardous event (OUMA & TATEISHI, 2014), like a flood, happens, the damage depends upon the factors affecting the flood, and vary from one study area to another (ELKHRACHY, 2015). Based on past investigations and reliable expert opinions seven causative factors were chosen to calculate a composite flood hazard index in the present study due to their significance in causing a flood. The factors considered were: runoff, slope, drainage density, soil type, distance to main channel, LULC, surface roughness. The chosen parameters have been demonstrated as powerful when incorporated into important research studies. The seven parameters were considered for mapping and were handled in the GIS environment, later the thematic maps were visualized independently. The following are the parameters used in the study.

Elevation surface and slope. Elevation surface considered in this study i.e., Digital Elevation Model (DEM) and slope play a vital part in governing the stability of a landscape. The amount of surface drainage reaching a site is greatly influenced by the slope direction. Highly vulnerable sites to flood occurrences events (OUMA & TATEISHI, 2014) have low gradient slopes when compared to high gradient slopes. In this study, contours were digitized at 10 m intervals from Survey of India topographical maps. The slope map was prepared from slope generation tools using the DEM generated from the contours in model builder. Classes of slope are assigned a higher rank with less value as they refer to flat terrain, while the ones with maximum value were ranked lower due to relatively high runoff (KUMAR ET AL., 2014).

Drainage density. The runoff from all the parts of the drainage basin is accumulated by streams and is dependent on the stream length keeping other factors constant. This means that less rainfall intensity implies lower runoff with low drainage density. The higher the catchment area is susceptible to erosion, resulting in sedimentation (OUMA & TATEISHI, 2014). Statistically, drainage density is the ratio of the total stream length of all the stream orders within a drainage basin to the area of that basin projected to the horizontal (DIXON ET AL., 2016). High-density values are favored in land surface with weak infiltration, where rainfall does not readily sinks therefore causing a good amount of runoff.

Distance to the main channel. A property, open space domain or roadway is subject to flooding if the flow carrying capacity of an adjacent or nearby drain or roadside drainage channel is frequently exceeding to overflow. Often the inundation emanates from riverbeds and expands into the surroundings. The role of the riverbed decreases as the distance increases. By considering the drainage network of the study area, the main channel, which has the maximum stream order, causes great damage. Hence, areas located close to the main channel and flow accumulation path are more likely to get flooded (ELKHRACHY, 2015).

Soil type. Soil texture is one of the critical components of soils, posing a great effect on flooding. For example, sandy soil absorbs water soonest, resulting in few runoffs. On the other hand, clay soils are less permeable and hold water longer than sandy soils. This suggests that areas characterized by clay soils are more influenced by flooding. For the study, soil types found within the municipality were considered in three broad categories: sandy loam, clay loam, sandy clay loam. The soil type that has the capacity to generate high flood rates is ranked high while the one with low capacity is ranked as 1 (OUMA & TATEISHI, 2014).

Land use. Land use portrays the appearance of the landscape, which reflects its utilization, condition, development and occasional phenology. Land cover like the vegetation cover of soils, has an important impact on the ability of the soil to act as a water store event, this determines that LULC is one of the crucial factors in deciding the probabilities of a flood occurrence event (OUMA & TATEISHI, 2014). Rainwater resulting in runoff is substantially more likely on barren fields than on those with a decent crop cover. Then again, impermeable surfaces, for example, concrete, ingest

no water and acts as a resistant cover, lessening the water hold up time, and increasing the peak discharge of water that enhances a peak flooding.

Surface roughness. The roughness of the earth's surface (e.g., roads, ground) and the objects there (e.g., buildings, vegetation) in terms of hydrodynamic friction is considered as one of the essential inputs for flood simulations. Inundation area by flood increases as channel surface roughness becomes higher (DORN ET AL., 2014). During the hydrodynamic simulation of the study, the roughness parameter is defined through the Manning's formula (CHOW, 1959) as shown in Table 2.

3. Results and discussions

Considering the contour map (Fig. 3a), the Digital Elevation Model (DEM) of the study area was created where the elevations of the terrain varied from 250 to 330 m as shown in Fig. 3b, while the slope percentage values range from 0.002 to 4.1 as shown in Fig. 3c. The highly elevated areas are shown in blue. The higher the elevation the greater is the runoff. The flow direction raster was created from DEM using the Arc Hydro extension and is shown in Fig. 4a. The raster gives the course in which inlet water will flow out of a cell with regards to its surrounding cells, showing the steepest heading from a cell to the surrounding cells.

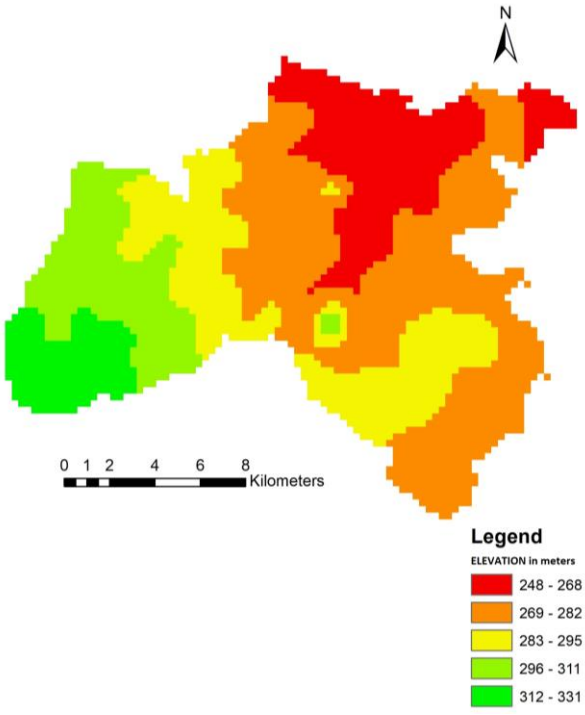

Fig. 3b. DEM extracted from contour map

3.1. Digital river network extraction

Extraction of watershed features from DEM is considered an important task in any hydrological study. In this study, Arc Hydro tools were used to extract stream networks (Fig. 4b). Flow direction is given as an input raster to basin function, to derive all the connected cells that come from the same drainage basin (ELKHRACHY, 2015). The entire study area is divided into 4 sub basins and the basin map is shown in Fig. 4c.

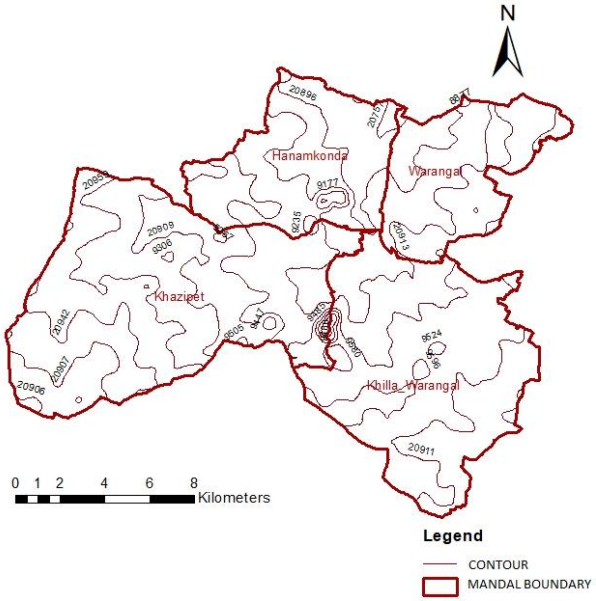

Fig. 3a. Contour map with 10 m contour interval

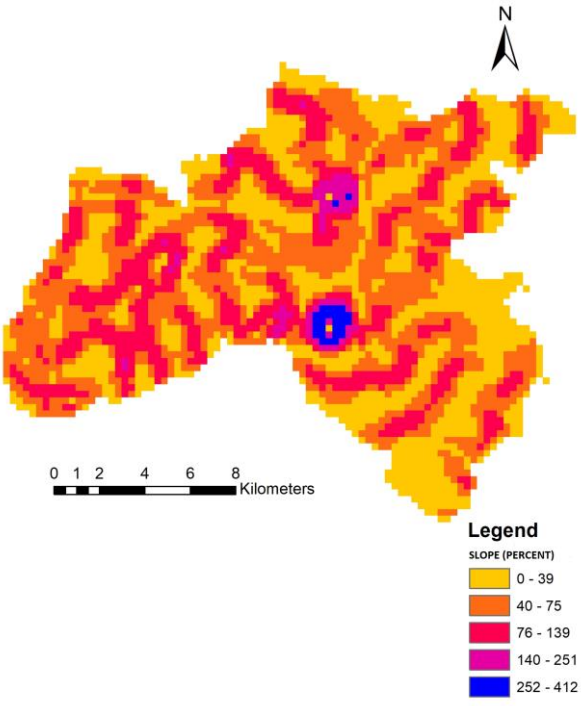

Fig. 3c. Slope map showing the percentage of slope

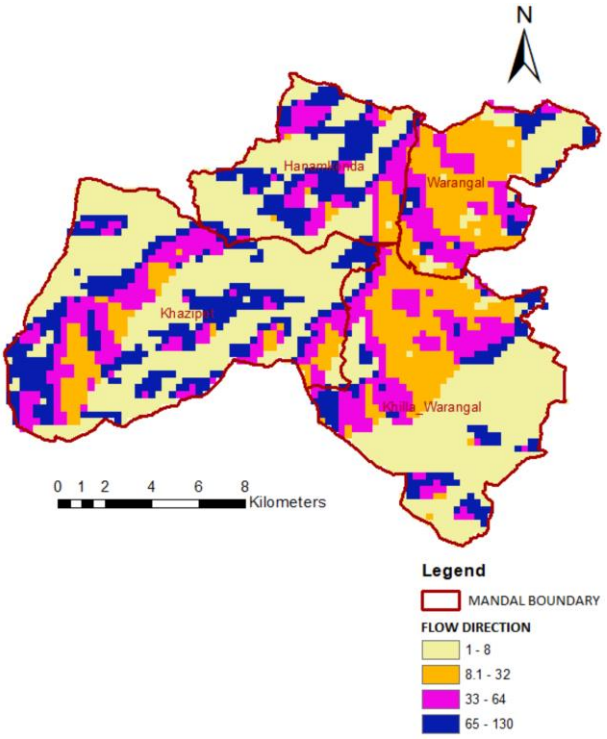

Fig. 4a. Flow direction map

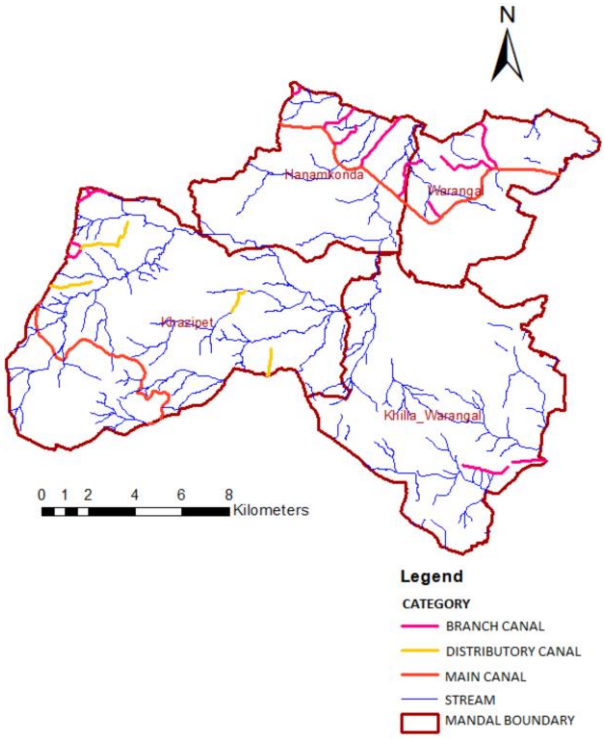

Fig. 4b. Streams delineated

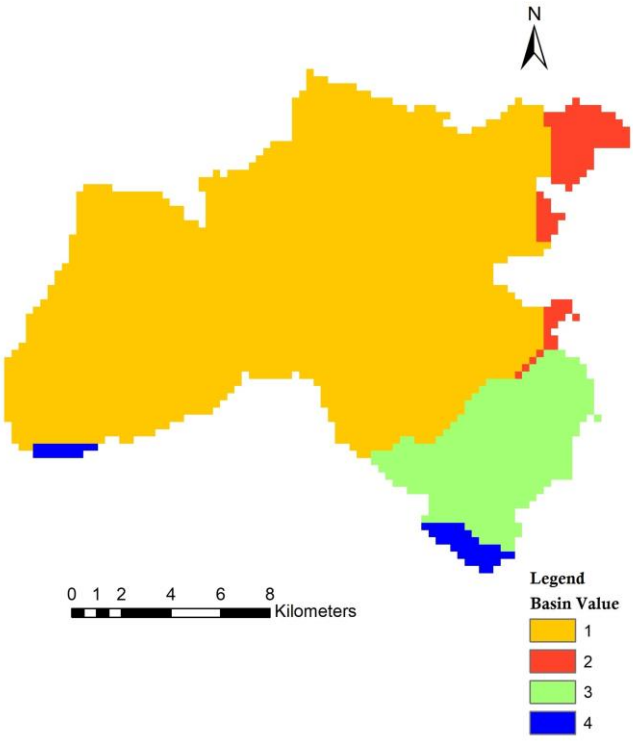

Fig. 4c. Basins in the study area

3.2. Calculation of distance to main channel

The proximity tool was used to calculate the zones that are near to the main channel. As the distance of the floodwater to reach the channel increases, the time taken to reach the channel also increases and hence the infiltration capacity increases. As shown in Fig. 5 the villages falling within the parts marked in blue are at high risk as the runoff in that area takes a longer time to the reach the main channel. The areas falling within the parts marked in yellow are at low risk of flooding.

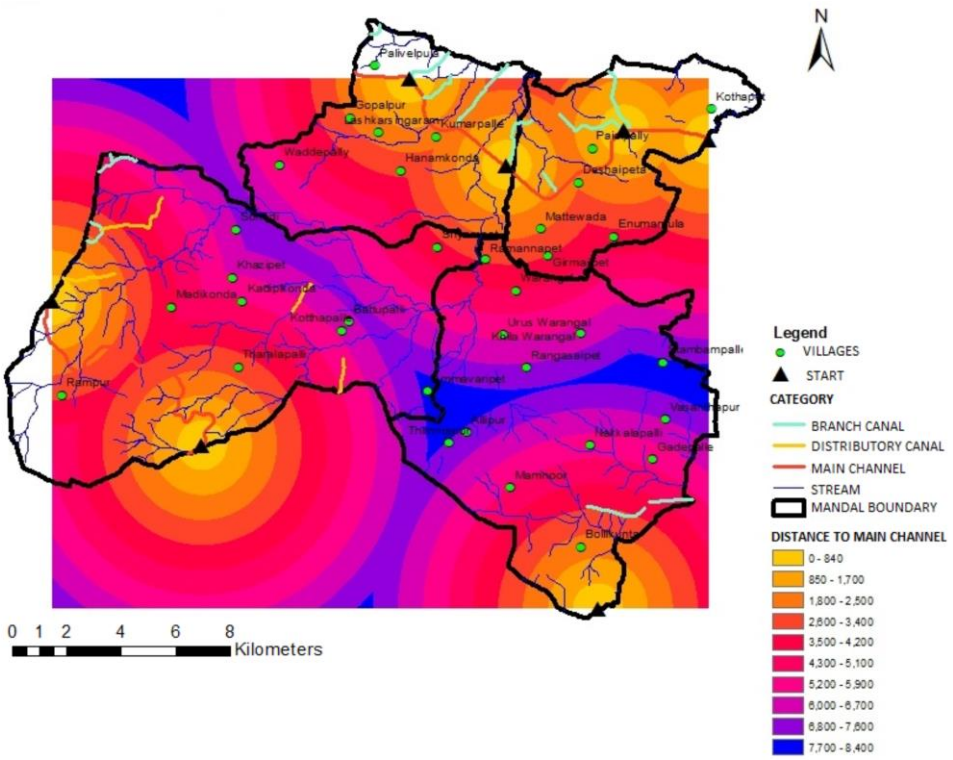

Fig. 5. Raster map of the distance to the main channel

3.3. Classification of land use and land cover (LULC)

LULC mapping of the WMC urban catchment was carried out using the Landsat satellite image for September 2005. ERDAS IMAGINE was used to process the data; a subset of the image was created based on the Area of Interest (AOI). The maximum likelihood algorithm was used for the supervised classification of the images, per-pixel signatures were assigned to the satellite data and the area was differentiated into four classes based on the corresponding Digital Number (DN) value of the different landscape elements. The classified LULC map is shown in Fig. 6. The results of the classification i.e., the areas and their percentages are given in Table 1. The observations made after classification of the WMC study area are that agricultural land was about 82% and built up area was 11%, wasteland occupies 4.16% and water bodies cover 2.3% of the area.

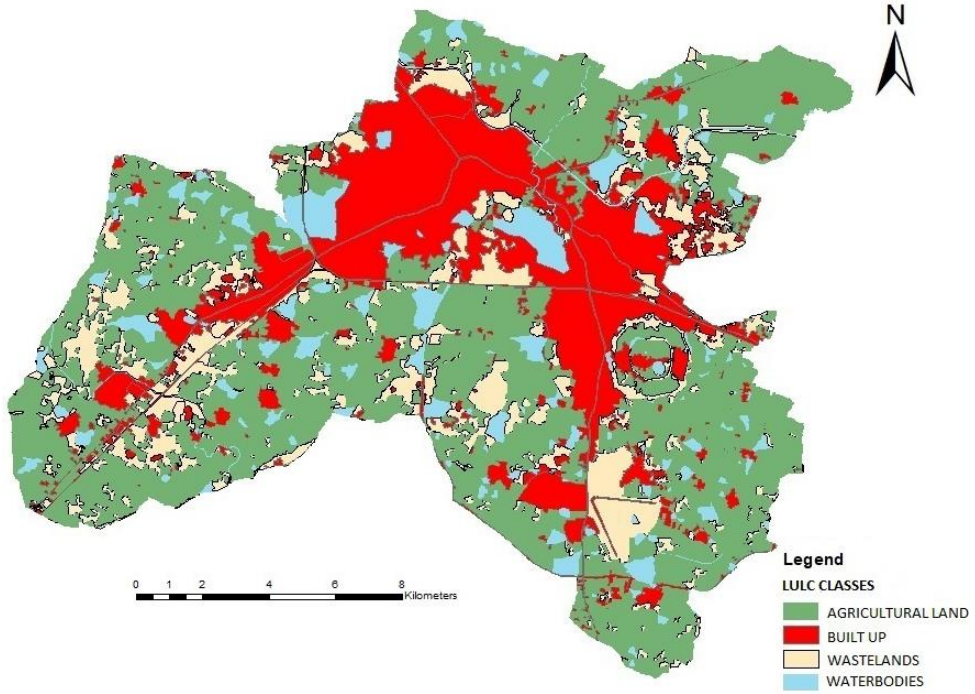

Fig. 6. LULC derived for the study area

Table 1. Table showing different LULC classes and their respective areas

Classes	Area (km²)	Percentage (%)
Built up	0.011085	11.172
Agricultural land	0.081684	82.33112
Wastelands	0.004129	4.161711
Waterbodies	0.002316	2.334348
Total	0.099214	100

3.4. Estimation of surface roughness value

The two multiple feature layers i.e. soil raster (Fig. 7) and the LULC raster were overlaid as input features in ArcGIS in order to combine the polygons and create an output spatial set representing a merged raster. The Manning's roughness coefficient (n) is commonly used to represent surface roughness. The appropriate Manning's 'n' value for each polygon of the soil-land map was assigned according to Table 2 and a roughness map was created as shown in Fig. 8.

Table 2. Estimated land use and surface roughness values for the study area

Classes	Manning's Roughness Coefficient
Built up	0.10
Agricultural land	0.05
Wastelands	0.03

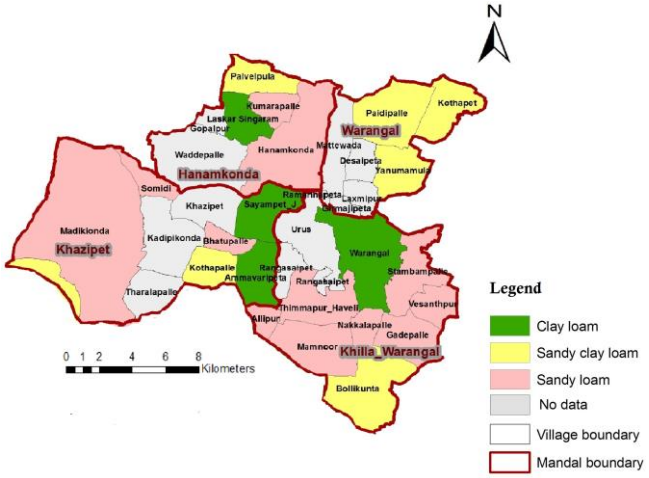

Fig. 7. Soil types present in the study area

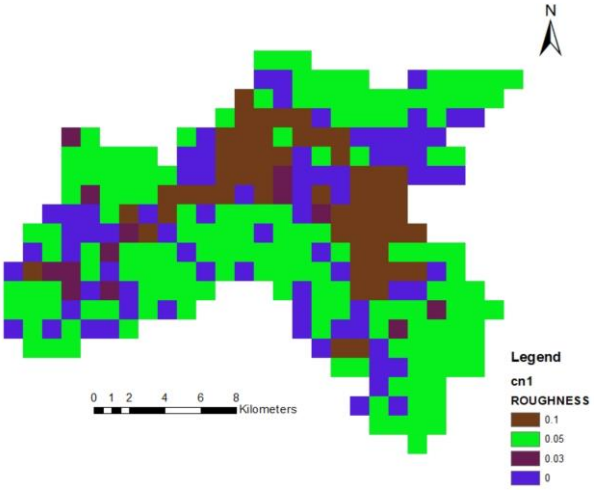

Fig. 8. Surface roughness map

3.5. Simulation of runoff using QSWAT

SWAT is a watershed model capable of simulating long period yields to find its effect on land management practices. Surface runoff in QSWAT was determined using the Soil Conservation Service Curve Number (SCS-CN) method while the potential evapotranspiration was determined by the Penmen-Moneith method. The central part of the SWAT model is water balance, the basic equation is:

PREC-SURQ - GW- PET - ET -SW = WYLD (Eq. 1)

Where,

PREC - Amount of precipitation in mm
SURQ - Amount of surface runoff in mm
GW - Groundwater contribution in mm
PET - Potential evapotranspiration in mm
ET - Actual evapotranspiration in mm
WYLD - Water yield (mm of H_2O)
SW - Soil water content (mm).

To derive runoff parameters, before simulation there are some pre-requisite requirements to be prepared that are available in the QSWAT directory. All the spatial data (DEM, Land use and Soil raster) were projected into a geographical coordinate system, WGS_1984_UTM_Zone_44N. Derived land use and soil look up tables were prepared. Climate data such as precipitation, solar radiation, wind speed and relative humidity were considered for the years 1995 to 2005. Once the data was ready for use, the model divided the whole drainage basin into 113 sub-catchments that were linked together with reference to many outlets. The layer of sub-catchments was divided as shown in Fig. 9.

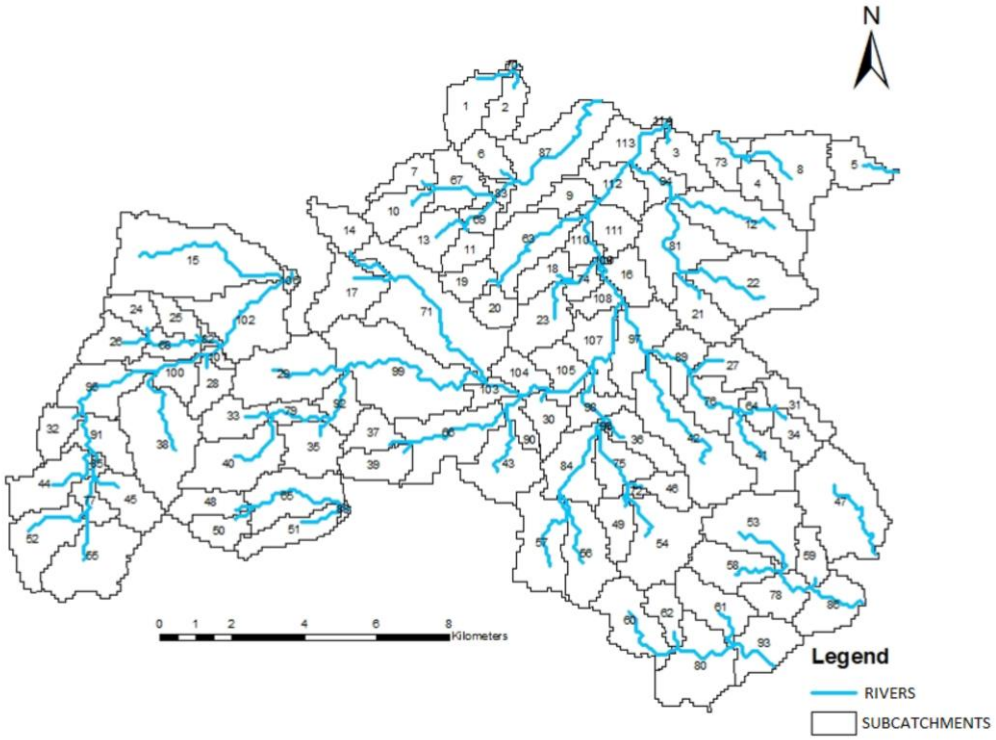

Fig. 9. The derived sub-catchments of the drainage line

3.6. Computing sub-basin parameters by using QSWAT and run-off model descriptions

From Table 1, it was observed that the study area was classified into four classes namely agricultural land, wasteland, built up land and water bodies. Using QSWAT Ref 2012.mdb file, a SWAT Code was assigned to each land-use and copied to the Excel file Watershed_Landuse.xls file. Similarly, from the soil type raster an Excel file Watershed_soils.xls file was created. The weather data such as precipitation (mm), temperature (^{0}C), wind velocity (m/s) and solar radiation (MJ/m^2) for the weather station nearest to the study area was downloaded from http://globalweather.tamu.edu site. Then all the results were copied to the WGEN_WatershedGan.xls file. The simulated results were obtained, once the SWAT was run successfully. It gave all the hydrological components such as average amount of precipitation, potential evapotranspiration, actual precipitation, groundwater contribution, surface runoff, soil water content, water yield for each sub basin and Curve Number (CN). For each sub-basin, a Curve Number value that is a part of yielding run-off volumes was assigned based on the class of LULC and hydrological soil type. Based on combinations of the Soil Conservation Service (SCS) land-use data and soil data for urban catchments (NATIONAL ENGINEERING HANDBOOK, 1972) CNs are listed in Table 3.

Table 3. List of curve number for urban catchments

Land use group	Hydrological category			
	A	B	C	D
Built up	47	65	76	82
Agricultural land	64	75	82	85
Wasteland	77	86	94	98

For the meteorological modeling, the QSWAT run was carried out using a rainfall monthly time series from the year 1995 to 2005. The rainfall for the month of September 2005, which had the peak rainfall, is shown in Fig. 10. Drainage intensity for any area is shown in Fig. 11 and was obtained by dividing total drainage length by the zone area. The drainage network covers sub-catchments 109, 96, 85, 103, 73, 4, 46 intensely in the figure, where corresponding drainage intensity values for the sub catchments were 87.04, 73, 40.6, 26.9, 20.2, 18.4, 7.8 km/km^2 respectively. Maximum intensity of drainage value was found to be for the zone 109, which indicated that it is more likely to risk due to flooding.

As per the output, sub-catchment 4 had the highest value for surface runoff. The sub-catchment 4 falls in wasteland in the LULC with a CN value of 96.5, it had a peak precipitation of 471.6 mm and a peak surface runoff of 309.289 mm (as shown in Fig. 12).

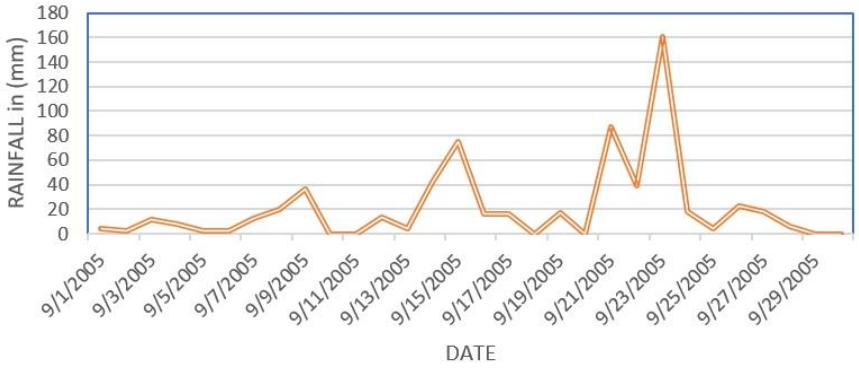

Fig. 10. Daily rainfall intensity in the month of September 2005

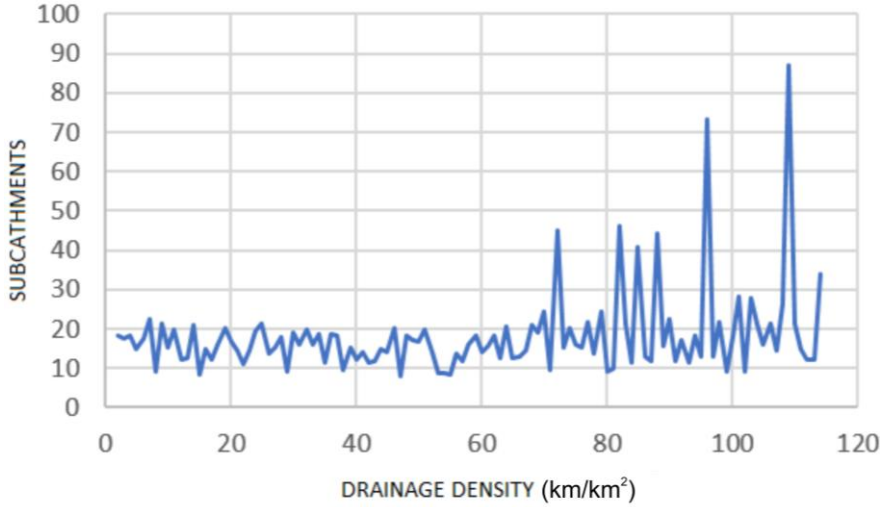

Fig. 11. Drainage density in the respective sub-catchments

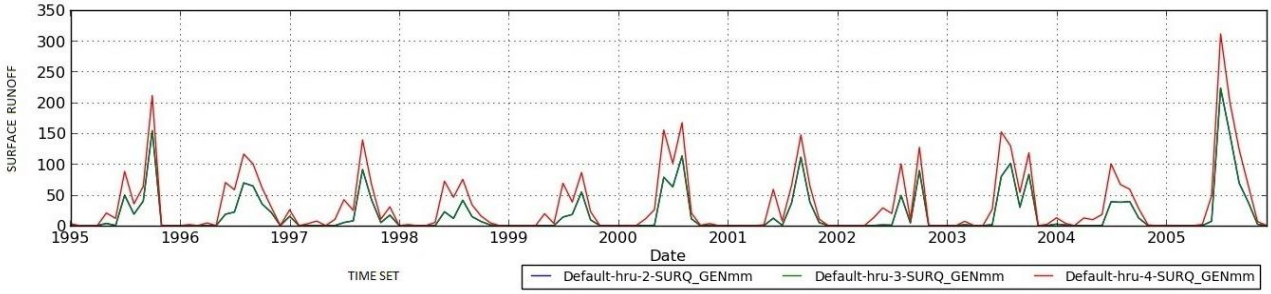

Fig. 12. Surface runoff generated in sub catchment 4 during time step

3.7. Sensitivity analysis, model calibration, model validation

Sensitivity analysis for the given model considered 13 parameters among which the surface water parameters were more sensitive to stream flow and were influencing hydrological parameters for the simulation. Calibration for water balance and stream flow was carried out for monthly data simulation. It was indicated by the base flow technique that about 60% of the total water yield at the outlet was found to be contributed by the surface runoff. The twelve most sensitive flow parameters were considered for calibration and their values differed iteratively inside the admissible limits until a satisfactory agreement was achieved between measured and simulated streamflow, which in turn improved the model efficiency significantly. When compared to measured flow data, the thorough hydrological calibration came about by great SWAT predictive efficiency at the monthly time step of the study area. It was found that the model, after validation, has a strong predictive capability with r^2, E_{NS} and D values of 0.65, 0.69 and 3.00, respectively.

3.8. Flood hazard mapping

In order to site the flood risk zones in Warangal city, an essential choice of factors such as run-off, slope percentage type of soil, surface roughness, drainage density, LULC and distance to main channel and the relative weights of the factors were ascertained. The weight of each factor was

given based on its estimated significance in causing flooding as described in Table 4. A multi-criterion evaluation was performed for the weights determined and the constraints map for each factor, utilizing the specific weights, was used to produce a flood hazard map. Final weighted flood hazard index was created as per Equation 2 from an additive model.

$$FHI = \sum_{i=1}^{n} (RIW_i).(RIW_j) \qquad \text{(Eq. 2)}$$

Where,
FHI = Flood hazard index
n= 2 (level of decision factors).

The consequences of a pairwise comparison matrix of the analysis are displayed in Table 5. Initially a single pair-wise comparison matrix (ELKHRACHY, 2015) was made for each criteria considered, by multiplying the values in each row together and calculating the nth base of the said causative factor (here n = 7, as 7 criteria are considered). Then, nth root of the factors was standardized to make a priority vector for the fitting weights. Finally, the Flood Hazard Index (FHI) was processed by utilizing the raster calculator in ArcMap using Equation 2. The acquired estimations of the FHI were characterized into low, medium and high, thus creating a Flood Hazard Map as shown in Fig. 13. The natural breaks method was used to classify the study area into three classes based on their hazard values. The zonal statistics function was used to define zones likely to be affected by flash flooding, and the classification scheme is summarized in Table 6 and the results are described as such, where 36 zones were deemed vulnerable to low flood risk, 27 zones vulnerable to moderate flood risk, 37 zones were highly vulnerable to flood risk. From Fig. 13 and previous considerations, it is clear that mostly, the high risk and the moderate risk areas were in the basin with relatively high curve numbers, drainage density and surface slope.
FHI= (Runoff X 0.355) + (Soil type X 0.240) + (Slope X 0.159) + (Roughness X0.104) + (Flow Accumulation X 0.068) + (Distance to main channel X 0.045) + (Land Use X 0.30).

Table 4. Drainage factors and their corresponding weights

Causative factor	Weight
Runoff	7
Soil type	6
Slope	5
Drainage density	4
Roughness	3
Distance to main channel	2
Land use	1

Table 5. Relative importance weights (RIWs) for factor criteria and Pairwise comparison matrix

Factor criteria	Runoff	Soil type	Slope	Drainage density	Roughness	Distance to main channel	LULC	Priority vector
Runoff	1	2	3	4	5	6	7	0.355
Soil type	0.5	1	2	3	4	5	6	0.240
Slope	0.33	0.5	1	2	3	4	5	0.159
Drainage density	0.25	0.33	0.50	1	2	3	4	0.104
Roughness	0.20	0.25	0.33	0.5	1	2	3	0.068
Distance to main channel	0.17	0.20	0.25	0.33	0.5	1	2	0.045
LULC	0.14	0.17	0.20	0.25	0.33	0.5	1	0.030

Table 6. Zones, which are affected by flood

FHI range	Hazard classification	No of sub-catchments likely to be affected
923–1050	Low	36
1060–1160	Moderate	27
1170–1280	High	32

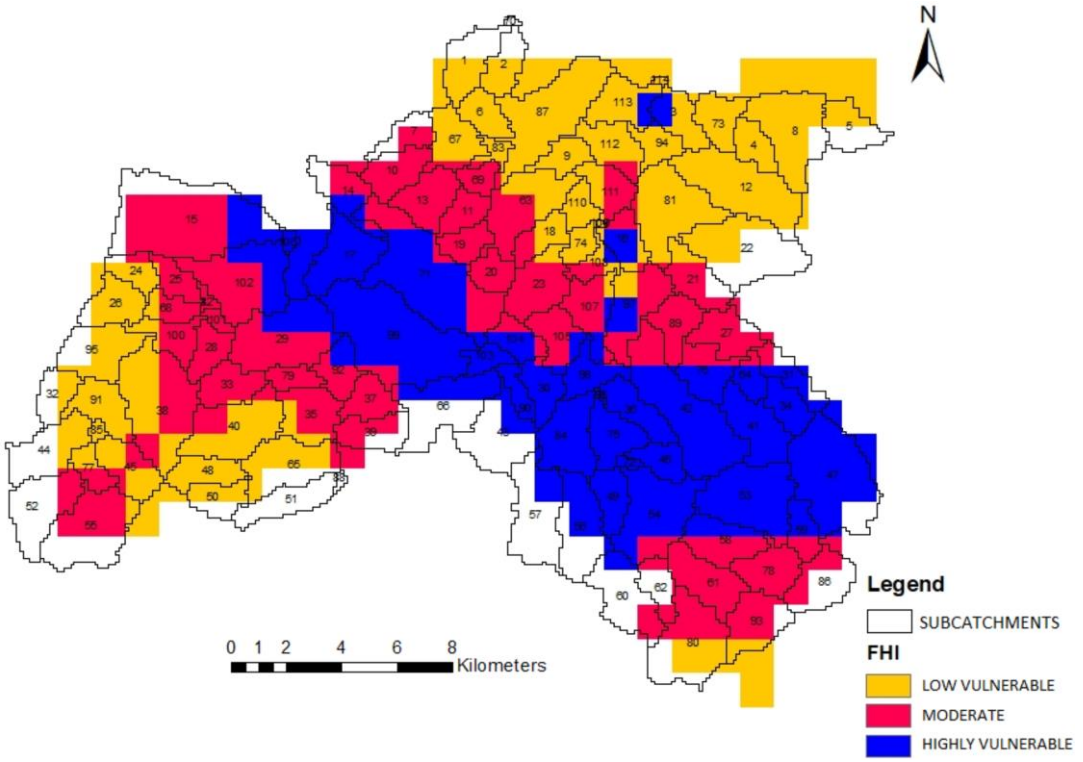

Fig. 13. Flood hazard map for the study area

4. Conclusions

In this investigation, the Analytic Hierarchy Process integrated with GIS was effectively connected in simulating the flood vulnerable zones for Warangal. GIS demonstrated significant possibilities in fighting disasters like floods. The social and monetary misfortunes caused by flood events, technological emergencies, as well as worldwide epidemics are increasing; requiring more powerful cooperative choice making when vulnerable. The study considered an additive model used to create the Flood Hazard Index, with the integration of GIS and spatial data. In developing this model, seven variables were considered (runoff, type of soil, slope percentage, surface roughness, flow accumulation, distance to main channel in the stream network, land use). SWAT, a 2D hydraulic model was used to create rainfall-runoff processes with the purpose of recreating the impacts of considered rainfall situations. The AHP process was utilized to create a hierarchal decision approach, in determining the relative weight of flood causative factors to derive a Flood Hazard Index map. The village administrative boundary was then overlain on the flood hazard map for each village, which is highly prone to flooding. Wadepally, Somidi, Khazipet, Kadipikonda, Battupalli, Kotthapalle, Ammavaripet, Ramanapet, Khilla Warangal, Nakkalpalli and Vasanthapur all fall within the high-risk zone. The benefits of this applied technique are found in the abilityto incorporate precision, its practical application, advanced yields, and its capacity to keep running for other situations. This study had never been done before, so subsequently, it is suggested that the accomplished outcomes would be useful in the administrative planning of Warangal city, and that this approach can be connected to every other city. It will also help with post-disaster activaties to evaluate harm and misfortune caused because of a surge. Some recommendations that are to be addressed in the study are:

1. Inadequacies of the available data, as some of the rainfall data from rain gauges was absent which led to consideration of only the rainfall data that was available.
2. The very recent DEM was used that was created by accurate measurement techniques and high spatial resolution satellite imagery.

References

Alaghmand S., Bin-Abdullah R., Abustan I., Vosoogh B. 2010. GIS-based River Flood Hazard Mapping in Urban Area: A Case Study in Kayu Ara River Basin, Malaysia. *International Journal of Engineering & Technology*, 2: 488–500.

Aldescu G.C. 2008. The necessity of flood risk maps on Timis river. *IOP Conference Series: Earth and Environmental Science*, 4. IOP Publishing.

Black A.R., Burns J.C. 2002. Re-assessing the flood risk in Scotland. *Science of the Total Environment,* 294, 1: 169–184.

Chen Y-R., Yeh C-H., Yu B. 2011. Integrated application of the analytic hierarchy process and the geographic information system for flood risk assessment and flood plain management in Taiwan. *Natural Hazards*, 59, 3: 1261–1276.

Chow V. 1959. *Open-Channel Hydraulics.* McGraw-Hill Book Company.

Correia F.N., Da Graça Saraiva M., Da Silva F.N., Ramos I. 1999. Floodplain management in urban developing areas. Part I. Urban Growth Scenarios and land-use controls. *Water Resources Management*, 13, 1: 1–21.

De Sherbinin A., Levy M., Adamo S., MacManus K., Yetman G., Mara V., Razafindrazay L., Goodrich B., Srebotnjak T., Aichele C. 2012. Migration and risk: net migration in marginal ecosystems and hazardous areas. *Environmental Research Letters*, 7, 4: 045602.

Dewan A.M., Monirul Islam M., Kumamoto T., Nishigaki M. 2007. Evaluating flood hazard for land-use planning in greater Dhaka of Bangladesh using remote sensing and GIS techniques. *Water Resources Management*, 21, 9: 1601–1612.

Dixon K.W., Lanzante J.R., Nath M.J., Hayhoe K., Stoner A., Radhakrishnan A., Balaji V., Gaitán C.F. 2016. Evaluating the Stationarity Assumption in Statistically Downscaled Climate Projections: Is Past Performance an Indicator of Future Results? *Climate change*, 135,395-408.

Dorn H., Vetter M., Höfle B. 2014. GIS-Based Roughness Derivation for Flood Simulations: A Comparison of Orthophotos, LiDAR and Crowdsourced Geodata, *Remote Sensing*., 6; 1739-1759.

Elkhrachy I. 2015. Flash Flood Hazard Mapping Using Satellite Images and GIS Tools: A case study of Najran City, Kingdom of Saudi Arabia (KSA). *The Egyptian Journal of Remote Sensing and Space Sciences*, 18, 2: 261–278.

Emmanouloudis D., Myronidis D., Ioannou K. 2008. Assessment of flood risk in Thasos Island with the combined use of multicriteria analysis AHP and geographical information system. *Innovative Applications Information Agricultural Environment*. 2: 103–115.

Fernández D.S., Lutz M.A. 2010. Urban flood hazard zoning in Tucumán Province, Argentina, using GIS and Multi Criteria Decision Analysis. *Engineering Geology*, 111, 1–4: 90–98.

Forte F., Pennetta L., Strobl R.O. 2005. Historic records and GIS applications for flood risk analysis in the Salento peninsula (southern Italy). *Natural Hazards and Earth System Sciences*, 5, 6: 833–844.

Gerl T., Bochow M., Kreibich H. 2014. Flood Damage Modeling on the basis of Urban Structure Mapping Using High-Resolution Remote Sensing Data. *Water*, 6, 8: 2367–2393.

Jaafari A., Najafi A., Pourghasemi H.R., Rezaeian J., Sattarian A. 2014. A GIS-based frequency ratio and index of entropy models for landslide susceptibility assessment in the Caspian forest, northern Iran. *International Journal of Environmental Science and Technology*, 11, 4: 909–926.

Koehler K.A., Volckens J. 2011. Prospects and pitfalls of occupational hazard mapping: 'between these lines there be dragons', *Annals of Occupational Hygiene*, 55, 8: 829–840.

Koelle H. 1975. Zur Berucksichtingung von interdependenzen bei Entscheidung sprozessen. *Analysen und Prognosen uber die Welt von Morgen*, 7.

Kumar T., Gautam A.K., Kumar T. 2014. Appraising the accuracy of GIS-based Multi-criteria decision-making technique for delineation of Groundwater potential zones. *Water Resources Management*, 28, 13: 4449.

Liu Y.B., Gebremeskel S., De Smedt F., Hoffmann L., Pfister, L. 2003. A diffusive transport approach for flow routing in GIS-based flood modeling. *Journal of Hydrology*, 283, 1–4: 91–106.

Mansor S., Shariah M., Billa L., Setiawan I., Jabar F. 2004. Spatial technology for natural risk management. *Disaster Prevention and Management.* 13, 5: 364–373.

Meja-Navarro M., Wohl E.E., Oaks S.D. 1994. Geological hazards, vulnerability, and risk assessment using GIS: model for Glenwood Springs, Colorado. *Geomorphology*, 10, 1–4: 331–354.

Meyer V., Scheuer S., Haase D. 2009. A multicriteria approach for flood risk mapping exemplified at the Mulde river, Germany. *Natural Hazards*, 48, 1: 17–39.

National Engineering Handbook, 1972. Design hydrographs, NEH Notice Section 4 Hydrology, 21: 4-102.

Ologunorisa T.E. 2003. An assessment of flood vulnerability zones in the Niger delta, Nigeria. *International Journal of Environmental Studies*, 61, 1: 31–38.

Ouma Y.O., Tateishi R. 2014. Urban Flood Vulnerability and Risk Mapping Using Integrated Multi-Parametric AHP and GIS: Methodological Overview and Case Study Assessment. *Water,* 6, 6: 1515–1545.

Patel D.P., Srivastava P.K. 2013. Flood hazards mitigation analysis using remote sensing and GIS: Correspondence with town planning scheme. *Water Resources Management*, 27, 7: 2353–2368.

Sanyal J., Lu X. 2006. GIS-based flood hazard mapping at different administrative scales: a case study in Gangetic West Bengal. *Singapore Journal of Tropical Geography*, 27: 207–220.

Schumann A.H., Funke R., Schultz G.A. 2000. Application of a geographic information system for conceptual rainfall–runoff modeling. *Journal of Hydrology*, 240, 1–2: 45–61.

Sinha R., Bapalu G., Singh L., Rath B. 2008. Flood risk analysis in the Kosi river basin, north Bihar using multi-parametric approach of analytical hierarchy process (AHP). *Journal of the Indian Society of Remote Sensing*, 36, 4: 335–349.

Sowmya K., John C.M., Shrivasthava N.K. 2015. Urban flood vulnerability zoning of Cochin City, southwest coast of India, using Remote Sensing and GIS. *Natural Hazards*, 75, 2: 1271–1286.

Tehrany M.S., Pradhan B., Jebur M.N. 2013. Spatial prediction of flood susceptible areas using rule based decision tree (DT) and a novel ensemble bivariate and multivariate statistical models in GIS. *Journal of* Hydrology, 504: 69–79.

Tehrany M.S., Pradhan B., Jebur M.N., Neamah M. 2014. Flood susceptibility mapping using a novel ensemble weights-of-evidence and support vector machine models in GIS. *Journal of Hydrology*, 512: 332–343.

Vahidnia M.H., Alesheikh A.A., Alimohammadi A., Hosseinali F. 2010. A GIS-based neurofuzzy procedure for integrating knowledge and data in landslide susceptibility mapping. *Computers & Geosciences*, 36, 9: 1101–1114.

Van A.V.D., Logtmeijer C. 2005. Economic hotspots: visualizing vulnerability to flooding. *Natural Hazards.* 36, 1–2: 65–80.

Wang Y., Li Z., Tang Z., Zeng G. 2011. A GIS-based spatial multi-criteria approach for flood risk assessment in the Dongting Lake Region, Hunan, Central China. *Water Resources Management*, 25, 13: 3465–3484.

Zangemeister C. 1971. *Nutzwertanalyse in der Systemtechnik*, 4th ed. Wittemannsche Buchhandlung, Munchen.

Zerger A. 2002. Examining GIS decision utility for natural hazard risk modelling. *Environmental Modelling & Software*, 17, 3: 287–294.

Zhu G.N., Hu J., Qi J., Gu C.C., Peng J.H. 2015. An integrated AHP and VIKOR for design concept evaluation based on rough number. *Advanced Engineering Informatics*, 29, 3: 408–418.

https://earthexplorer.usgs.gov/

https://www.hexagongeospatial.com/products/power-portfolio/erdas-imagine

http://globalweather.tamu.edu